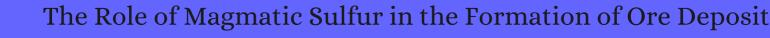
## CITATION REPORT List of articles citing



DOI: 10.2138/rmg.2011.73.16 Reviews in Mineralogy and Geochemistry, 2011, 73, 513-578.

Source: https://exaly.com/paper-pdf/50283460/citation-report.pdf

Version: 2024-04-09

This report has been generated based on the citations recorded by exaly.com for the above article. For the latest version of this publication list, visit the link given above.

The third column is the impact factor (IF) of the journal, and the fourth column is the number of citations of the article.

#	Paper	IF	Citations
116	High Cu concentrations in vapor-type fluid inclusions: An artifact?. <i>Geochimica Et Cosmochimica Acta</i> , <b>2012</b> , 88, 255-274	5.5	87
115	Fluid evolution of the Jiawula AgPbØn deposit, Inner Mongolia: mineralogical, fluid inclusion, and stable isotopic evidence. <b>2013</b> , 55, 204-224		51
114	An experimental study of the solubility of Gallium(III) oxide in HCl-bearing water vapour. <i>Geochimica Et Cosmochimica Acta</i> , <b>2013</b> , 119, 137-148	5.5	11
113	Solubility and partitioning behavior of Au, Cu, Ag and reduced S in magmas. <i>Geochimica Et Cosmochimica Acta</i> , <b>2013</b> , 112, 288-304	5.5	94
112	Degassing of CO2, SO2, and H2S associated with the 2009 eruption of Redoubt Volcano, Alaska. <b>2013</b> , 259, 270-284		72
111	Fluid-present melting of sulfide-bearing ocean-crust: Experimental constraints on the transport of sulfur from subducting slab to mantle wedge. <i>Geochimica Et Cosmochimica Acta</i> , <b>2013</b> , 110, 106-134	5.5	59
110	ReDs and UPb geochronology of porphyry Mo deposits in central Jilin Province: Mo ore-forming stages in northeast China. <b>2013</b> , 55, 1763-1785		30
109	Enrichment of Platinum-group Elements (PGE) and Re-Os Isotopic Tracing for Porphyry Copper (Gold) Deposits. <b>2014</b> , 88, 1288-1309		4
108	Isotopic fluid changes in a Neoproterozoic porphyry@pithermal system: The Uruguay mine, southern Brazil. <i>Ore Geology Reviews</i> , <b>2014</b> , 60, 146-160	3.2	7
107	Gold mineralization in the Guilaizhuang deposit, southwestern Shandong Province, China: Insights from phase relations among sulfides, tellurides, selenides and oxides. <i>Ore Geology Reviews</i> , <b>2014</b> , 56, 276-291	3.2	22
106	An experimental study of the solubility of MoO3 in aqueous vapour and low to intermediate density supercritical fluids. <i>Geochimica Et Cosmochimica Acta</i> , <b>2014</b> , 136, 169-193	5.5	27
105	A predictive model for the transport of copper by HCl-bearing water vapour in ore-forming magmatic-hydrothermal systems: Implications for copper porphyry ore formation. <i>Geochimica Et Cosmochimica Acta</i> , <b>2014</b> , 129, 33-53	5.5	35
104	SPb isotopic geochemistry, UPb and ReDs geochronology of the Huanggangliang FeBn deposit, Inner Mongolia, NE China. <i>Ore Geology Reviews</i> , <b>2014</b> , 59, 109-122	3.2	63
103	Metal (copper) segregation in magmas. <b>2014</b> , 208-209, 462-470		8
102	Fluid evolution of the Tongkuangyu porphyry copper deposit in the Zhongtiaoshan region: Evidence from fluid inclusions. <i>Ore Geology Reviews</i> , <b>2014</b> , 63, 498-509	3.2	26
101	Fluid/melt in continental deep subduction zones: Compositions and related geochemical fractionations. <b>2015</b> , 58, 1457-1476		23
100	Effects of temperature, silicate melt composition, and oxygen fugacity on the partitioning of V, Mn, Co, Ni, Cu, Zn, As, Mo, Ag, Sn, Sb, W, Au, Pb, and Bi between sulfide phases and silicate melt.  Geochimica Et Cosmochimica Acta. 2015. 162. 25-45	5.5	76

## (2017-2015)

99	The oxidation state, and sulfur and Cu contents of arc magmas: implications for metallogeny. <b>2015</b> , 233, 27-45		217
98	Ore metals beneath volcanoes. <b>2015</b> , 8, 168-170		8
97	The solubility of sulfur in hydrous basaltic melts. <i>Chemical Geology</i> , <b>2015</b> , 418, 104-116	4.2	16
96	Sulfur radical species form gold deposits on Earth. <b>2015</b> , 112, 13484-9		75
95	Toward a quantitative model for the formation of gravitational magmatic sulfide deposits. <i>Chemical Geology</i> , <b>2015</b> , 391, 56-73	4.2	19
94	Geochemical constraints on CuBe and Fe skarn deposits in the Edong district, Middlellower Yangtze River metallogenic belt, China. <i>Ore Geology Reviews</i> , <b>2015</b> , 64, 425-444	3.2	70
93	Relationships between arc maturity and CuMoAu porphyry and related epithermal mineralization at the Cenozoic Arasbaran magmatic belt. <i>Ore Geology Reviews</i> , <b>2015</b> , 65, 487-501	3.2	43
92	Ore-forming granites from Jurassic porphyry Mo deposits, eastBentral Jilin Province, China: geochemistry, geochronology, and petrogenesis. <b>2016</b> , 58, 1158-1174		16
91	Geology and age of the Morrison porphyry CuAuMo deposit, Babine Lake area, British Columbia. <b>2016</b> , 53, 950-978		1
90	Combined effect of carbon dioxide and sulfur on vaporllquid partitioning of metals in hydrothermal systems. <i>Geochimica Et Cosmochimica Acta</i> , <b>2016</b> , 187, 311-333	5.5	27
89	Structures and Acidity Constants of Silver-Sulfide Complexes in Hydrothermal Fluids: A First-Principles Molecular Dynamics Study. <b>2016</b> , 120, 8435-8443		6
88	Redox processes in subducting oceanic crust recorded by sulfide-bearing high-pressure rocks and veins (SW Tianshan, China). <b>2016</b> , 171, 1		25
87	Sulphate incorporation in monazite lattice and dating the cycle of sulphur in metamorphic belts. <b>2016</b> , 171, 1		19
86	Encyclopedia of Geochemistry. <b>2016</b> , 1-3		
85	Open-system behaviour of magmatic fluid phase and transport of copper in arc magmas at Krakatau and Batur volcanoes, Indonesia. <b>2016</b> , 327, 669-686		11
84	Links between arc volcanoes and porphyry-epithermal ore deposits. <b>2016</b> , 44, 11-14		24
83	Tempo of magma degassing and the genesis of porphyry copper deposits. <b>2017</b> , 7, 40566		75
82	Co-variability of S6+, S4+, and S2In apatite as a function of oxidation state: Implications for a new oxybarometer. <b>2017</b> , 102, 548-557		73

81	Normallto adakite-like arc magmatism associated with the El Abra porphyry copper deposit, Central Andes, Northern Chile. <b>2017</b> , 106, 2687-2711		10
80	Cu and Fe diffusion in rhyolitic melts during chalcocite dissolution[Implications for porphyry ore deposits and tektites. <b>2017</b> , 102, 1287-1301		14
79	Geochronology, geochemistry and SrNdHfBP isotopes of the Early Cretaceous Taoxihu Sn deposit and related granitoids, SE China. <i>Ore Geology Reviews</i> , <b>2017</b> , 89, 350-368	3.2	21
78	Isotopic (CDB) geochemistry and ReDs geochronology of the Haobugao ZnBe deposit in Inner Mongolia, NE China. <i>Ore Geology Reviews</i> , <b>2017</b> , 82, 130-147	3.2	25
77	Fe isotope fractionation between chalcopyrite and dissolved Fe during hydrothermal recrystallization: An experimental study at 350 LC and 500 bars. <i>Geochimica Et Cosmochimica Acta</i> , <b>2017</b> , 200, 87-109	5.5	24
76	Cu-rich porphyry magmas produced by fractional crystallization of oxidized fertile basaltic magmas (Sangnan, East Junggar, PR China). <i>Ore Geology Reviews</i> , <b>2017</b> , 91, 296-315	3.2	9
75	Cu-Mo partitioning between felsic melts and saline-aqueous fluids as a function of XNaCleq, fO2, and fS2. <b>2017</b> , 102, 1987-2006		21
74	Whole rock geochemistry, molybdenite Re-Os geochronology, stable isotope and fluid inclusion investigations of the Siah-Kamar deposit, western Alborz-Azarbayjan: New constrains on the porphyry Mo deposit in Iran. <i>Ore Geology Reviews</i> , <b>2017</b> , 91, 638-659	3.2	7
73	Sulfur isotopic zoning in apatite crystals: A new record of dynamic sulfur behavior in magmas. <i>Geochimica Et Cosmochimica Acta</i> , <b>2017</b> , 215, 387-403	5.5	16
72	Amphibole and apatite insights into the evolution and mass balance of Cl and S in magmas associated with porphyry copper deposits. <b>2017</b> , 172, 1		45
71	Visible and InvisibleIforms of gold and silver in the crystallization products of melts in the FeBIAgIAu system: experimental data. <b>2017</b> , 474, 636-640		3
70	Geology, mineralogy and evolution of iron skarn deposits in the Zanjan district, NW Iran: Constraints from U-Pb dating, Hf and O isotope analyses of zircons and stable isotope geochemistry. <i>Ore Geology Reviews</i> , <b>2017</b> , 84, 42-66	3.2	7
69	Early Cretaceous porphyry copper mineralization in Northeast China: the Changfagou example. <b>2017</b> , 59, 185-203		9
68	Molybdenite ReDs age, HDCSBb isotopes, and fluid inclusion study of the Caosiyao porphyry Mo deposit in Inner Mongolia, China. <i>Ore Geology Reviews</i> , <b>2017</b> , 81, 728-744	3.2	27
67	Late Jurassic Sn metallogeny in eastern Guangdong, SE China coast: Evidence from geochronology, geochemistry and Sr队d册fB isotopes of the Dadaoshan Sn deposit. <i>Ore Geology Reviews</i> , <b>2017</b> , 83, 63-83	3.2	20
66	Subsurface deposition of Cu-rich massive sulphide underneath a Palaeoproterozoic seafloor hydrothermal systemEhe Red Bore prospect, Western Australia. <b>2018</b> , 53, 1061-1078		2
65	Genetic links between porphyry Mo and peripheral quartz vein Mo <b>t</b> u mineralization in the Baituyingzi district, eastern Inner Mongolia, NE China. <b>2018</b> , 165, 305-327		4
64	Sulfur diffusion in dacitic melt at various oxidation states: Implications for volcanic degassing. <i>Geochimica Et Cosmochimica Acta</i> , <b>2018</b> , 226, 50-68	5.5	9

## (2020-2018)

63	New contributions to the understanding of Kiruna-type iron oxide-apatite deposits revealed by magnetite ore and gangue mineral geochemistry at the El Romeral deposit, Chile. <i>Ore Geology Reviews</i> , <b>2018</b> , 93, 413-435	3.2	28
62	S isotopic geochemistry, zircon and cassiterite upb geochronology of the Haobugao Sn polymetallic deposit, southern Great Xinglin Range, NE China. <i>Ore Geology Reviews</i> , <b>2018</b> , 93, 168-180	3.2	22
61	Origin of Early Cretaceous A-type granite and related Sn mineralization in the Sanjiaowo deposit, eastern Guangdong, SE China and its tectonic implication. <i>Ore Geology Reviews</i> , <b>2018</b> , 93, 60-80	3.2	20
60	Magmatic sulphides in Quaternary Ecuadorian arc magmas. <b>2018</b> , 296-299, 580-599		22
59	Geochronology, geochemistry, and zircon Hf isotopes of the Mo-bearing granitoids in the eastern Jilin-Heilongjiang provinces, NE China: Petrogenesis and tectonic implications. <b>2018</b> , 53, 877-898		3
58	Elevated Magmatic Sulfur and Chlorine Contents in Ore-Forming Magmas at the Red Chris Porphyry Cu-Au Deposit, Northern British Columbia, Canada. <b>2018</b> , 113, 1047-1075		45
57	Diffusion of molybdenum and tungsten in anhydrous and hydrous granitic melts. 2018,		
56	Fluid-controlled element transport and mineralization in subduction zones. <b>2018</b> , 3, 87-104		8
55	Resource assessment of undiscovered seafloor massive sulfide deposits on an Arctic mid-ocean ridge: Application of grade and tonnage models. <i>Ore Geology Reviews</i> , <b>2018</b> , 102, 818-828	3.2	7
54	Sulfides in alkaline and peralkaline rocks: textural appearance and compositional variations. <b>2018</b> , 195, 155-175		3
53	Influence of eruptive style on volcanic gas emission chemistry and temperature. 2018, 11, 678-681		16
52	An experimental calibration of a sulfur-in-apatite oxybarometer for mafic systems. <i>Geochimica Et Cosmochimica Acta</i> , <b>2019</b> , 265, 242-258	5.5	22
51	Discussion on Au transportation mechanism in melt-magma-fluid in porphyry Cu deposit IA case study from Jinchang porphyry Au (Cu) deposit, Heilongjiang province, China. <i>Ore Geology Reviews</i> , <b>2019</b> , 111, 102968	3.2	0
50	Geo-fO2: Integrated Software for Analysis of Magmatic Oxygen Fugacity. <b>2019</b> , 20, 2542		7
49	Structurally bound S2[IS1[IS4+, S6+ in terrestrial apatite: The redox evolution of hydrothermal fluids at the Phillips mine, New York, USA. <i>Ore Geology Reviews</i> , <b>2019</b> , 107, 1084-1096	3.2	15
48	Constraints on the formation of the Baogutu reduced porphyry copper deposit (West Junggar, NW China): Assessing the role of mafic magmas in mineralization. <b>2019</b> , 336-337, 112-124		O
47	The origin of variable-180 zircons in Jurassic and Cretaceous Mo-bearing granitoids in the eastern Xing Meng Orogenic Belt, Northeast China. <b>2019</b> , 61, 129-149		3
46	Spectroscopic, Raman, EMPA, Micro-XRF and Micro-XANES Analyses of Sulphur Concentration and Oxidation State of Natural Apatite Crystals. <b>2020</b> , 10, 1032		8

45	Mineralization Age and Hydrothermal Evolution of the Fukeshan Cu (Mo) Deposit in the Northern Great Xingan Range, Northeast China: Evidence from Fluid Inclusions, HDBP Isotopes, and ReDs Geochronology. <b>2020</b> , 10, 591		2
44	The Geochemistry of Magnetite and Apatite from the El Laco Iron Oxide-Apatite Deposit, Chile: Implications for Ore Genesis. <b>2020</b> , 115, 1461-1491		8
43	A review of magnetite geochemistry of Chilean iron oxide-apatite (IOA) deposits and its implications for ore-forming processes. <i>Ore Geology Reviews</i> , <b>2020</b> , 126, 103748	3.2	7
42	Sulfur in New Zealand geothermal systems: insights from stable isotope and trace element analyses of anhydrite from Rotokawa and Ngatamariki geothermal fields, Taupo Volcanic Zone. <b>2020</b> , 1-17		2
41	Petrologic Reconstruction of the Tieshan Magma Plumbing System: Implications for the Genesis of Magmatic-Hydrothermal Ore Deposits within Originally Water-Poor Magmatic Systems. <b>2020</b> , 61,		8
40	Factors controlling Pt <b>P</b> d enrichments in intracontinental extensional environment: Implications from Tongshankou deposit in the Middlellower Yangtze River Metallogenic Belt, Eastern China. <i>Ore Geology Reviews</i> , <b>2020</b> , 124, 103621	3.2	3
39	Settling of Immiscible Droplets: A Theoretical Model for the Missing Link Between Microscopic and Outcrop Observations. <b>2020</b> , 125, e2019JB018829		2
38	Zircon geochemistry of Edong granitoids in the Middle-Lower Yangtze Metallogenic Belt (Eastern China): Constraints on W-Cu-Fe skarn mineralization. <i>Ore Geology Reviews</i> , <b>2020</b> , 120, 103461	3.2	3
37	Volatile transport of metals and the Cu budget of the active White Island magmatic-hydrothermal system, New Zealand. <b>2020</b> , 398, 106905		4
36	Early Cretaceous bimodal magmatism related epithermal mineralization: A case study of the Gaosongshan gold deposit in the northern Lesser Xinglin Range, NE China. <i>Ore Geology Reviews</i> , <b>2020</b> , 121, 103563	3.2	4
35	Effects of sulfide composition and melt H2O on sulfur content at sulfide saturation in basaltic melts. <i>Chemical Geology</i> , <b>2021</b> , 559, 119913	4.2	3
34	Geological and Sr-Nd-S-Pb isotopic constraints on the genesis of the Baiyinchagan tin polymetallic deposit, southern Great Xing' an Range, China. <b>2021</b> , 37, 1731-1748		1
33	The sulfur concentration at anhydrite saturation in silicate melts: Implications for sulfur cycle and oxidation state in subduction zones. <i>Geochimica Et Cosmochimica Acta</i> , <b>2021</b> , 306, 98-123	5.5	О
32	Variable modes of formation for tonalite-trondhjemite-granodiorite-diorite (TTG)-related porphyry-type Cu   Au deposits in the Neoarchean southern Abitibi subprovince (Canada): Evidence from petrochronology and oxybarometry.		2
31	Magmatic constraints on the Ermi porphyry copper mineralization, Northeast China: Evidence from zircon U-Pb geochronology, whole-rock geochemistry and Sr-Nd-Hf isotopic geochemistry. <i>Ore Geology Reviews</i> , <b>2021</b> , 136, 104294	3.2	1
30	Instrumental mass fractionation during sulfur isotope analysis by secondary ion mass spectrometry in natural and synthetic glasses. <i>Chemical Geology</i> , <b>2021</b> , 578, 120318	4.2	2
29	Sulfur Content at Sulfide Saturation of Peridotitic Melt at Upper Mantle Conditions. 2021,		О
28	Chemical Enrichment of Precious Metals in Iron Sulfides Using Microwave Energy. 623-629		1

27	Encyclopedia of Geochemistry. <b>2018</b> , 303-305		1
26	Cenozoic orogenic gold system in Tibet. <b>2020</b> , 36, 1315-1353		12
25	Magmatic Controls on Porphyry Copper Genesis. 2012,		12
24	Increasing sulfur and chlorine contents in ore-forming magmas: The key to Pulang porphyry Cu-Au formation, SW China. <i>Ore Geology Reviews</i> , <b>2021</b> , 139, 104518	3.2	2
23	<del>IIII IIII IIII IIII IIII IIII IIII II</del>		
22	In-situ SPb isotopic and trace elemental compositions of sulfides from the Habo Au polymetallic deposit: Evidences for vein-type Au mineralization in the Ailaoshan Au belt. <i>Ore Geology Reviews</i> , <b>2021</b> , 140, 104583	3.2	
21	An ab-initio study on the thermodynamics of disulfide, sulfide, and bisulfide incorporation into apatite and the development of a more comprehensive temperature, pressure, pH, and composition-dependent model for ionic substitution in minerals. <b>2022</b> ,		
20	Sulfide and sulfate saturation of dacitic melts as a function of oxygen fugacity. <i>Geochimica Et Cosmochimica Acta</i> , <b>2022</b> ,	5.5	1
19	In situ SrD isotopic and elemental compositions of apatite and zircon from Pengcuolin granodiorites: implications for Jurassic metallogenic variation in the southern Tibet. <i>Ore Geology Reviews</i> , <b>2022</b> , 104869	3.2	О
18	Timing and ore formation of the Xiaokele porphyry Cu (Mo) deposit in the northern Great Xing In Range, NE China: Constraints from geochronology, fluid inclusions, and HDBP isotopes. <i>Ore Geology Reviews</i> , 2022, 143, 104806	3.2	O
17	Geological features and ore-forming mechanisms of the Chating CuAu deposit: A rare case of porphyry deposit in the MiddleIlower Yangtze River metallogenic belt. <i>Ore Geology Reviews</i> , <b>2022</b> , 144, 104860	3.2	1
16	Redox-controlled chalcophile element geochemistry of the Polaris Alaskan-type mafic-ultramafic complex, British Columbia, Canada. <i>Canadian Mineralogist</i> , <b>2021</b> , 59, 1627-1660	0.7	O
15	New Potential Sphalerite, Chalcopyrite, Galena and Pyrite Reference Materials for Sulfur Isotope Determination by Laser Ablation-MC-ICP-MS. <i>Geostandards and Geoanalytical Research</i> ,	3.6	О
14	Origin of the Dongbulage MoBbIn deposit in the Great Hinggan Range, northeast China: Geological, molybdenite ReIDs dating, fluid inclusion, and CHIDSIP isotope constraints. <i>Ore Geology Reviews</i> , <b>2022</b> , 147, 104991	3.2	O
13	A general ore formation model for metasediment-hosted Sb-(Au-W) mineralization of the Woxi and Banxi deposits in South China. <i>Chemical Geology</i> , <b>2022</b> , 121020	4.2	1
12	Sulfur dissolution capacity of highly hydrated and fluid-saturated dacitic magmas at the lower crust and implications for porphyry deposit formation. <i>Geochimica Et Cosmochimica Acta</i> , <b>2022</b> , 333, 107-123	5.5	Ο
11	Fluid inclusions and CHDBP isotope systematics of the Senj Mollu deposit, Alborz magmatic belt, northern Iran: implications for fluid evolution and regional mineralization. 1-21		
10	The effects of pressure, fO2, fS2 and melt composition on the fluidfhelt partitioning of Mo: Implications for the Mo-mineralization potential of upper crustal granitic magmas. <b>2022</b> ,		

9	SO2 solubility and degassing behavior in silicate melts. <b>2022</b> , 336, 150-164	1
8	Contrasting geochemical signatures between fertile and barren granites and multi-isotope (SrNdPbBHe) study in the LamasuBaibo deposit, NW China: Implications for petrogenesis and ore genesis. 2022, 149, 105114	O
7	UNDERSTANDING Cu DEFICIENCY AND Mo ENRICHMENT IN THE JURASSIC ZHANGGUANGCAI-LESSER XINGAN CONTINENTAL ARC (NE CHINA): INSIGHTS FROM THE LUMING PORPHYRY MO DEPOSIT.	Ο
6	Metallogenesis of Porphyry Copper Deposit Indicated by In Situ Zircon U-Pb-Hf-O and Apatite Sr Isotopes. <b>2022</b> , 12, 1464	Ο
5	The role of immiscible sulfides for sulfur isotope fractionation in arc magmas: Insights from the Talkeetna island arc crustal section, south-central Alaska. <b>2023</b> , 121325	Ο
4	A newly synthesized reference material for in situ sulfur isotope measurement of sphalerite using laser ablation MC-ICP-MS.	O
3	Anhydrite solubility enhanced by CaO in silicate melts: Implications for sulfur cycling in subduction zones. <b>2023</b> , 349, 135-145	O
2	Pre-eruptive water content and volatile degassing processes in the southern Okinawa Trough magma: Implications for subduction zone water recycling and magmatic contributions to hydrothermal systems. <b>2023</b> , 446-447, 107145	O
1	Fluid evolution, metal source, and ore genesis of sulfide mineralization, Nim Ka Thana Copper Belt, Rajasthan, India: evidence from mineral chemistry, fluid inclusions and sulfur isotope geochemistry. <b>2023</b> , 16,	0